Journal of Bacteriology

Biotechnology | Full-Length Text

Dissecting structure and function of the monovalent cation/H^+ antiporters Mdm38 and Ylh47 in *Saccharomyces cerevisiae*

Masaru Tsujii,[1] Ellen Tanudjaja,[1] Haoyu Zhang,[1] Haruto Shimizukawa,[1] Ayumi Konishi,[1] Tadaomi Furuta,[2] Yasuhiro Ishimaru,[1] Nobuyuki Uozumi[1]

AUTHOR AFFILIATIONS See affiliation list on p. 12.

ABSTRACT *Saccharomyces cerevisiae* Mdm38 and Ylh47 are homologs of the Ca^{2+}/H^+ antiporter Letm1, a candidate gene for seizures associated with Wolf-Hirschhorn syndrome in humans. Mdm38 is important for K^+/H^+ exchange across the inner mitochondrial membrane and contributes to membrane potential formation and mitochondrial protein translation. Ylh47 also localizes to the inner mitochondrial membrane. However, knowledge of the structures and detailed transport activities of Mdm38 and Ylh47 is limited. In this study, we conducted characterization of the ion transport activities and related structural properties of Mdm38 and Ylh47. Growth tests using Na^+/H^+ antiporter-deficient *Escherichia coli* strain TO114 showed that Mdm38 and Ylh47 had Na^+ efflux activity. Measurement of transport activity across *E. coli*-inverted membranes showed that Mdm38 and Ylh47 had K^+/H^+, Na^+/H^+, and Li^+/H^+ antiport activity, but unlike Letm1, they lacked Ca^{2+}/H^+ antiport activity. Deletion of the ribosome-binding domain resulted in decreased Na^+ efflux activity in Mdm38. Structural models of Mdm38 and Ylh47 identified a highly conserved glutamic acid in the pore-forming membrane-spanning region. Replacement of this glutamic acid with alanine, a non-polar amino acid, significantly impaired the ability of Mdm38 and Ylh47 to complement the salt sensitivity of *E. coli* TO114. These findings not only provide important insights into the structure and function of the Letm1-Mdm38-Ylh47 antiporter family but by revealing their distinctive properties also shed light on the physiological roles of these transporters in yeast and animals.

IMPORTANCE The inner membrane of mitochondria contains numerous ion transporters, including those facilitating H^+ transport by the electron transport chain and ATP synthase to maintain membrane potential. Letm1 in the inner membrane of mitochondria in animals functions as a Ca^{2+}/H^+ antiporter. However, this study reveals that homologous antiporters in mitochondria of yeast, Mdm38 and Ylh47, do not transport Ca^{2+} but instead are selective for K^+ and Na^+. Additionally, the identification of conserved amino acids crucial for antiporter activity further expanded our understanding of the structure and function of the Letm1-Mdm38-Ylh47 antiporter family.

KEYWORDS *S. cerevisiae*, cation/H^+ antiporter, mitochondria, yeast

As the major cation in cytoplasm and organelles, potassium (K^+) contributes to the formation of the electric potential component ΔΨ and to osmotic regulation (1–3). Since the inner mitochondrial membrane has a relatively high negative charge of −150 to −180 mV, K^+ enters the mitochondrial matrix at a constant rate, which increases osmotic pressure and swelling of mitochondria (4). Mitchell proposed that ΔpH across the inner mitochondrial membrane formed by electron transfer would drive K^+/H^+ antiporter-mediated K^+ extrusion from the matrix to avoid mitochondrial swelling (5). Leucine zipper/EF-hand-containing transmembrane protein 1 (Letm1), a well-known

Editor Julie A. Maupin-Furlow, University of Florida Department of Microbiology and Cell Science, Gainesville, Florida, USA

Address correspondence to Nobuyuki Uozumi, uozumi@tohoku.ac.jp.

The authors declare no conflict of interest.

See the funding table on p. 12.

Received 1 May 2024
Accepted 9 July 2024
Published 31 July 2024

candidate gene for seizure development in Wolf-Hirschhorn syndrome in humans, contributes to cation/H^+ antiport across the inner mitochondrial membrane in many organisms (6–15). A genome-wide RNA interference screen identified Letm1 as a Ca^{2+}/H^+ antiporter in *Drosophila* (7). In a knockdown strain of *Drosophila Letm1*, mitochondria are swollen and fragmented (8). Similarly, human Letm1 prevents mitochondrial swelling by Ca^{2+}/H^+ antiport across the inner mitochondrial membrane (9–11). Knockdown of human *Letm1* significantly reduces respiratory oxygen consumption and ATP production (12). In addition, Letm1 is important for early embryonic development and survival in mice (13). In *Caenorhabditis elegans*, knockdown of Letm1 causes disorganized mitochondrial morphology and large variations in diameter (14). In *Trypanosoma brucei*, silencing of Letm1 results in mitochondrial swelling, and the phenotype can be complemented by the addition of nigericin, a K^+/H^+ exchanger ionophore (15). These reports suggest that Ca^{2+}/H^+ antiport and/or K^+/H^+ antiport activity of Letm1 plays an important role in mitochondrial morphogenesis.

The *Saccharomyces cerevisiae* genome contains two genes that encode members of the same family as human Letm1 and *Drosophila* Letm1, called Mdm38 (YOL027) and Ylh47 (YPR125) (16). Mdm38 is known to be involved in K^+/H^+ exchange across the inner mitochondrial membrane (17–22). In contrast to Letm1, the amino acid sequences of Mdm38 and Ylh47 do not contain an EF-hand sequence. An *mdm38* mutant strain shows delayed growth on glycerol medium and loss of mitochondrial membrane potential (17). Studies with K^+-sensitive and H^+-sensitive probes revealed that loss of *mdm38* abolishes K^+/H^+ exchange across the inner mitochondrial membrane (18) and causes mitochondrial swelling and induction of mitophagy (19). Nigericin complements the delayed growth of *mdm38*-defective strains, suggesting that Mdm38 contributes to K^+/H^+ antiport across the inner mitochondrial membrane to avoid mitochondrial swelling (22). Mdm38 also facilitates the translation of mitochondrial proteins and indirectly interacts with newly synthesized proteins via the ribosome (16). Mdm38 contains a C-terminal ribosome-binding domain (RBD), which binds to the ribosomal protein Mrp49 (16). Loss of *mdm38* significantly reduces the amounts of complexes III and IV in the respiratory chain (16). These results suggest that Mdm38 is important for both K^+/H^+ antiport and the biogenesis of respiratory chain complexes. However, the direct transport activities of Mdm38 and Ylh47 and their transport mechanism have not yet been elucidated.

In this study, we used functional complementation in an *E. coli* strain TO114, which has defective mutations in three kinds of Na^+/H^+ antiporters, NhaA, NhaB, and ChaA as well as characterization of the transport kinetics of yeast Mdm38 and Ylh47 (23). This *E. coli* expression system had been previously used to study the activities of several other transporters (24–26). Although *Drosophila* Letm1 and human Letm1 exchange Ca^{2+} for H^+ (7, 10, 11), we here show that yeast Mdm38 and Ylh47 transport K^+, Na^+, and Li^+ but not Ca^{2+}. Structural modeling and mutational analyses further revealed structurally important domains and identified the conserved glutamic acid essential for the activity of this cation/H^+ transporter family.

MATERIALS AND METHODS

Plasmid construction

The primers used for plasmid construction are listed in Table S1. The sequences encoding Mdm38 and Ylh47 without their N-terminal mitochondrial targeting signal were amplified by PCR using primer pairs pTrcHis2BMDM38F and pTrcHis2BMDM38R, and pTrcHis2BYLH47F and pTrcHis2BYLH47R, respectively. The coding region of NhaA was amplified by PCR with primer pair pTrcHis2BEcNhaAHisF and pTrcHis2BEcNhaAHisR. The 5′ and 3′ regions of the gene encoding Mdm38E152A were amplified by PCR with primer pairs pTrcHis2BMDM38F and MDM38_E152A_R, and MDM38_E152A_F and pTrcHis2BMDM38R, respectively. The 5′ and 3′ regions of the gene encoding Ylh47E150A were amplified by PCR with primer pairs pTrcHis2BYLH47F and YLH47_E150A_R, and YLH47_E150A_F and pTrcHis2BYLH47R, respectively. The genes encoding

Mdm38ΔRBD and Mdm38Δcc were amplified by primer pairs pTrcHis2BMDM38F and pTrcHis2BMDM38deltaRBDR, and pTrcHis2BMDM38F and pTrcHis2BMDM38deltaccR, respectively. Each PCR fragment was inserted into the *Pst*I site of pTrcHis2B using the In-Fusion HD Cloning Kit (Takara Bio Inc., Japan).

Growth assay conditions

The Na^+ efflux complementation assays with *E. coli* strain TO114 (W3110 *nhaA::Km*^{r} *nhaB::Em*^{r} *chaA::Cm*^{r}) were performed as previously described with slight modifications (24, 26). The *E. coli* mutants transformed with the empty vector (pTrcHis2B) or with pTrcHis2B containing Mdm38 or Ylh47 were grown overnight in KLB medium at 30°C with shaking at 150 rpm. Cells were harvested by centrifugations, washed, and resuspended in KLB medium, where 171 mM NaCl in LB medium was replaced by 100 mM KCl. Cell suspensions were adjusted to OD_{600} of 0.5 and serially diluted (1:10). Cell suspensions (5 µL) were spotted on KLB medium containing 10 or 100 µM of IPTG and either 0 or 25 mM NaCl. Plates were incubated at 30°C for 1 day. For the K^+ influx complementation assays, growth of *E. coli* strain Δ*dghu* (BW25113 Δ*trkG*Δ*trkH*Δ*kup*Δ*kdpA*) (27) transformed with either the empty vector (pTrcHis2B) or the vector containing Mdm38 or Ylh47 was tested under low K^+ conditions. Transformants were grown overnight in K^+ minimal medium (46 mM Na_2HPO_4, 23 mM NaH_2PO_4, 8 mM $(NH_4)_2SO_4$, 0.4 mM $MgSO_4$, 6 mM $FeSO_4$, 10 µg/mL thiamine, and 1% glucose) containing 30 mM KCl. The harvested cells were washed and resuspended in K^+ minimal medium. Cell suspensions were adjusted to OD_{600} of 0.5 and serially diluted (1:10) the same as for Na^+ efflux complementation assays. Cells were spotted on K^+ minimal medium containing 1µM of IPTG and 10, 20, or 30mM of KCl and incubated at 30°C for 2 days.

Cation/H^+ antiporter assay

Inverted membranes of *E. coli* TO114 were prepared as previously reported (24, 28). Briefly, 400–2,000 µg of inverted membranes was added to a buffer containing 10 mM Tris-HCl pH 8.0, 5 mM $MgCl_2$, 140 mM choline-Cl, and 1 µM acridine orange. An amount of 10 mM Tris-DL-lactate was added to initiate quenching of acridine orange fluorescence due to respiration. KCl, NaCl, LiCl, RbCl, or $CaCl_2$ was added when the fluorescence became stable. Furthermore, 70 s after adding the salt, 10 mM carbonyl cyanide m-chlorophenyl-hydrazone (CCCP) was added to collapse the ΔpH across the inverted membranes. Acridine orange fluorescence was measured at 525 nm with an excitation wavelength of 492 nm.

Sequence alignment of Letm1, Mdm38, and Ylh47

Multiple sequence alignment of Letm1, Mdm38, and Ylh47 was performed using Clustal Omega (29). Structural components, such as the mitochondrial targeting sequence (MTS), transmembrane region (TM), ribosome-binding domain, coiled-coil regions (CCs), and EF-hand, were defined based on the UniProtKB (https://www.uniprot.org/uniprotkb/, Letm1: O95202, Mdm38: Q08179, Ylh47: Q06493). In initial structural models of the Letm1-Mdm38-Ylh47 family, the AlphaFold structures of Letm1, Mdm38, and Ylh47 contained many disordered regions (multiple long loops). Furthermore, none of the structures displayed a configuration in which the MTS on the N-terminal side and the RBD on the C-terminal side were positioned on opposite sides of the membrane in the AlphaFold structures. Electron microscopy in previous studies suggested that the MTS and RBD were located on opposite sides of the membrane, and Letm1 forms a hexamer (10). Therefore, six RBDs were first arranged to make appropriate contacts, by aligning the C-terminal helices of the TM region (TM-C, residues after the conserved Glu in the RBD) similar to residues T19-V27 of the HIV-1 capsid hexamer (PDB: 5HGL; a representative structure with perpendicular helices in the center) (30). Then, each N-terminal helical part of the TM region was linked manually to the TM-C so that it was perpendicular to the membrane, thus completing the structure of TM-RBD of the Letm1-Mdm38-Ylh47 family.

Note that the MTS and the CCs appeared to have helical-like structures, but since their orientation was unknown, modeling of these domains was not part of this study.

Statistical analysis

GraphPad Prism10 was used for statistical analysis. Two-tailed Student's *t* test was used to analyze significant differences between the two groups.

RESULTS

Mdm38 and Ylh47 have Na^+ efflux activity but not K^+ uptake activity

To determine the ion transport activities of Mdm38 and Ylh47, we used expression in *E. coli* since this method is suitable for analysis of ion transport of endosomal membrane proteins from eukaryotes (31). The genes encoding Mdm38 and Ylh47 but without their N-terminal mitochondrial targeting sequence were expressed in *E. coli* strain TO114. Growth of the transformants was tested on medium with and without the addition of 25 mM NaCl. The strain expressing Mdm38 showed delayed growth in the presence of 100 µM IPTG; therefore, we performed the growth assays in media with either 10 or 100 µM IPTG (Fig. 1A and B). Transformants containing the empty vector did not grow in the presence of 25 mM NaCl, while NhaA, an Na^+/H^+ antiporter from *E. coli*, complemented the Na^+ sensitivity of TO114 strains (Fig. 1A). *E. coli* expressing Mdm38 grew well in medium containing 25 mM NaCl and 10 µM IPTG. With 100 µM IPTG, the mutant containing Ylh47 grew in 25 mM NaCl-containing medium (Fig. 1B). These results suggested that Mdm38 and Ylh47 activity was able to exclude Na^+ from the cells. In addition, we tested K^+ influx activity of Mdm38 and Ylh47 using an *E. coli* strain, Δ*dghu,* carrying deletions in four K^+ uptake transporters (27) (Fig. 1C). Under control conditions, on K^+ minimal medium supplemented with 30 mM KCl, all transformants were able to grow. Transformants expressing KEA3, a chloroplast K^+/H^+ antiporter of *Arabidopsis thaliana,* grew in media containing 10 and 20 mM KCl (24), whereas *E. coli* containing Mdm38 and Ylh47 did not grow, suggesting that Mdm38 and Ylh47 did not have K^+ uptake activity.

Mdm38 and Ylh47 have cation/H^+ antiport activities

Cation/H^+ antiport activity of Mdm38 and Ylh47 was determined using inverted membranes of TO114 transformants to measure fluorescence dequenching of acridine orange due to H^+ efflux across the membrane after addition of various kinds of cations (Fig. 2) (24, 25). Addition of KCl to inverted membranes containing Mdm38 or Ylh47 resulted in a larger increase of acridine orange fluorescence compared to that of the control membranes (empty vector) (Fig. 2A). The same was seen when NaCl, LiCl, or RbCl instead of KCl was added to membranes from cells expressing Mdm38 or Ylh47 (Fig. 2B). In contrast, Mdm38 and Ylh47 had no detectable Ca^{2+}/H^+ antiport activity. To determine the affinity of Mdm38 and Ylh47 for transport of K^+ and Na^+, dequenching of acridine orange fluorescence was quantified at different concentrations of KCl and NaCl (Fig. 3). The K_m values of Mdm38 for KCl and NaCl were 4.57 ± 1.94 and 3.41 ± 2.07 mM, respectively, while those of Ylh47 were 4.79 ± 1.06 and 3.80 ± 1.19 mM, respectively (Table 1). The results suggest that Mdm38 and Ylh47 can function as Na^+/H^+, K^+/H^+, Li^+/H^+, and Rb^+/H^+ antiport systems but do not have Ca^{2+}/H^+ transport activity, which is different from Letm1.

Ribosome-binding domains are important for the antiport activity of Mdm38

Letm1, Mdm38, and Ylh47 contain several motifs: the MTS, a single transmembrane region, a ribosome-binding domain, and coiled-coil regions (Fig. 4A). While the RBD of Mdm38 is involved in mitochondrial protein translation, CCs are involved in mild heat adaptation on glycerol medium (20). To evaluate the impact of the RBD and the coiled-coil regions on the ion transport activity of Mdm38, we expressed Mdm38 variants lacking either the RBD (Mdm38 ΔRBD) or CCs (Mdm38 Δcc) in TO114 (Fig. 4B). Both

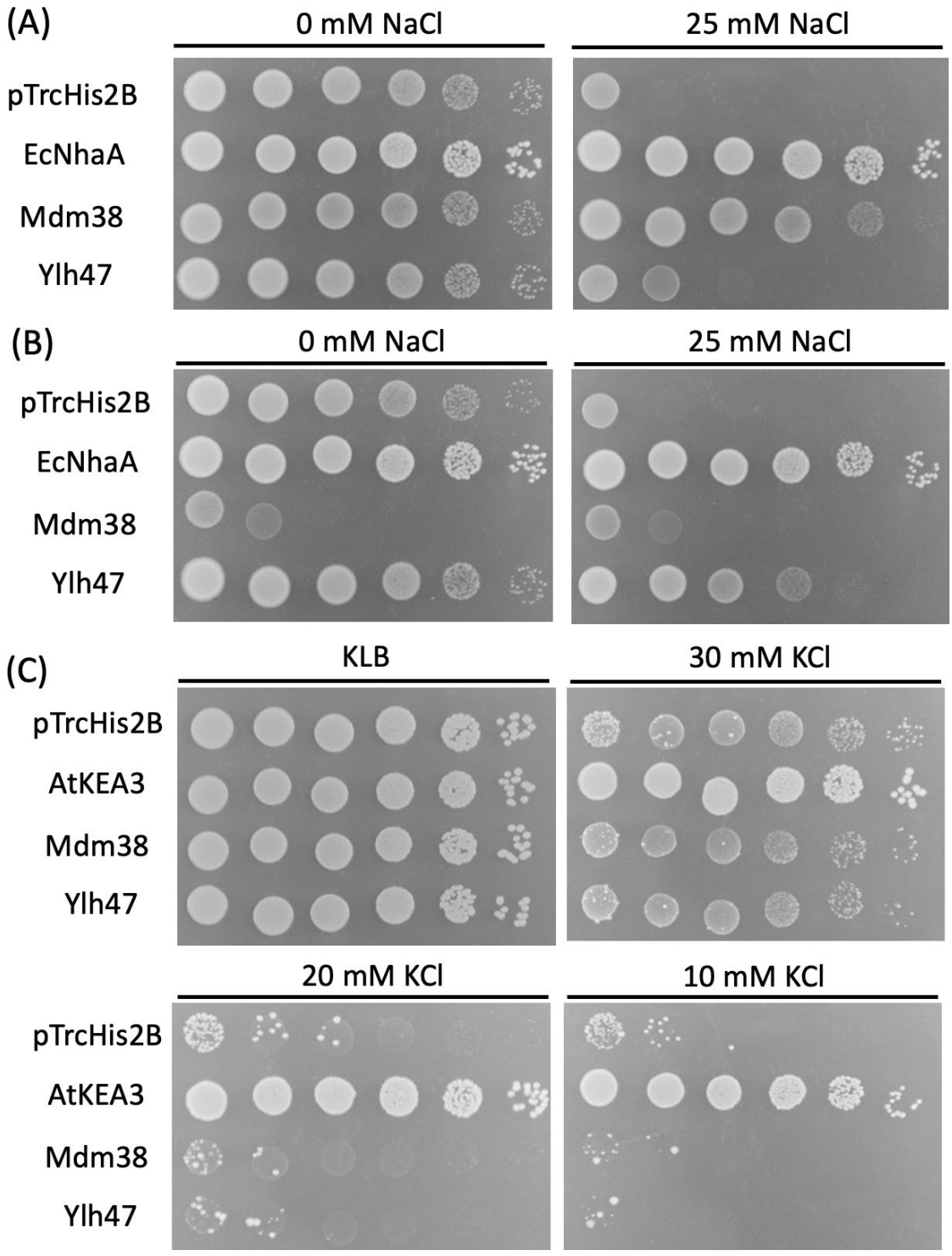

FIG 1 Growth of Na^+ efflux or K^+ uptake-deficient *E. coli* strains containing Mdm38 or Ylh47. (A and B) Complementation assay with Na^+/H^+ antiporter-deficient *E. coli* strain TO114 transformed with plasmids encoding EcNhaA, Mdm38, Ylh47, or the empty vector pTrcHis2B. Tenfold serial dilutions of the cells were spotted on KLB with 0 mM or 25 mM NaCl and 10 µM (A) or 100 µM (B) IPTG. A representative example of three biological replicates is shown. (C) Growth of K^+ uptake-deficient *E. coli* strain Δ*dghu* containing plasmids encoding AtKEA3, Mdm38, Ylh47, or the empty vector pTrcHis2B. Tenfold serial dilutions of the cells were spotted on KLB medium or K^+ minimal medium supplemented with 10, 20, or 30 mM KCl. A representative example of three biological replicates is shown.

Mdm38 and Mdm38Δcc complemented the growth of TO114 in medium containing 25 mM NaCl. However, Mdm38 ΔRBD failed to restore growth of TO114, suggesting that the RBD is required for the ion transport activity of Mdm38.

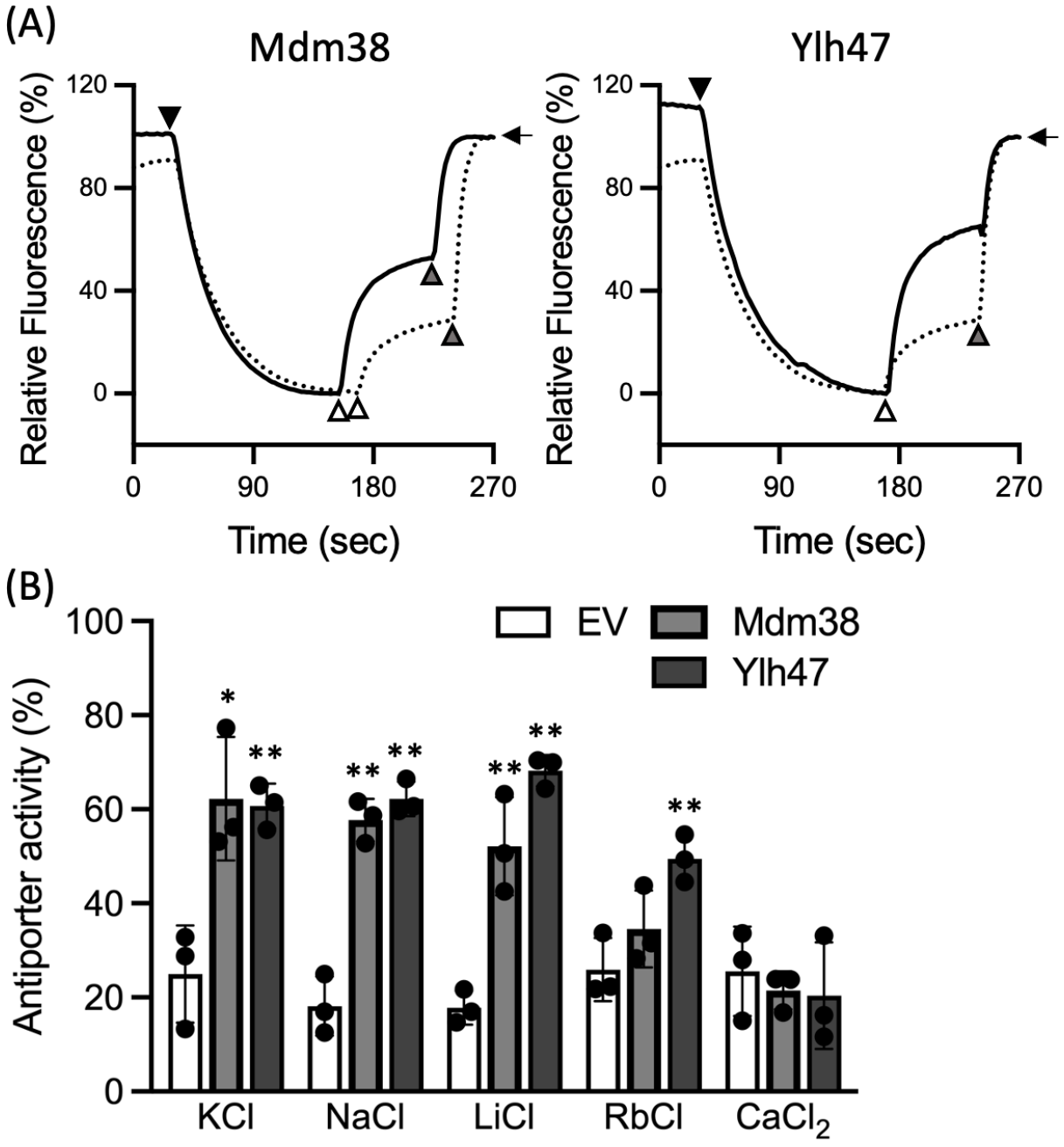

FIG 2 Cation/H^+ antiport activities of Mdm38 and Ylh47. (A) Determination of K^+/H^+ antiporter activities in inverted membranes by dequenching of acridine orange fluorescence. The closed triangle and open triangle indicate the time when L-lactate and KCl were added, respectively. Finally, CCCP was added (gray triangle) to collapse the ΔpH across the inverted membranes, and the filled arrow indicates when that was achieved. Solid lines represent the results with Mdm38 and Ylh47, and dashed lines indicate the data obtained with membranes isolated from TO114 containing the empty vector (EV). Traces shown are representative examples of three biological replicates. (B) Determination of K^+, Na^+, Li^+, Rb^+, and Ca^{2+} transport activity of Mdm38 and YLH47. Assays were performed as for (A) but instead of KCl, NaCl, LiCl, RbCl, or $CaCl_2$ was added to the inverted membranes. Error bars represent SD (n = 3). The significance of differences between the control of *E. coli* TO114 with the EV and TO114 expressing Mdm38 and Ylh47 was analyzed by Students' t-test (**P < 0.01, *P < 0.05, n = 3).

A conserved glutamic acid residue in the transmembrane region of Mdm38 and Ylh47 is involved in the antiport activity

To gain an insight into the structure-function properties of Mdm38, Ylh47, and Letm1, we compared their amino acid sequences (Fig. 5; Fig. S1). Letm1, Mdm38, and Ylh47 have a well-conserved transmembrane region and RBD flanked by the MTS in the N-terminal

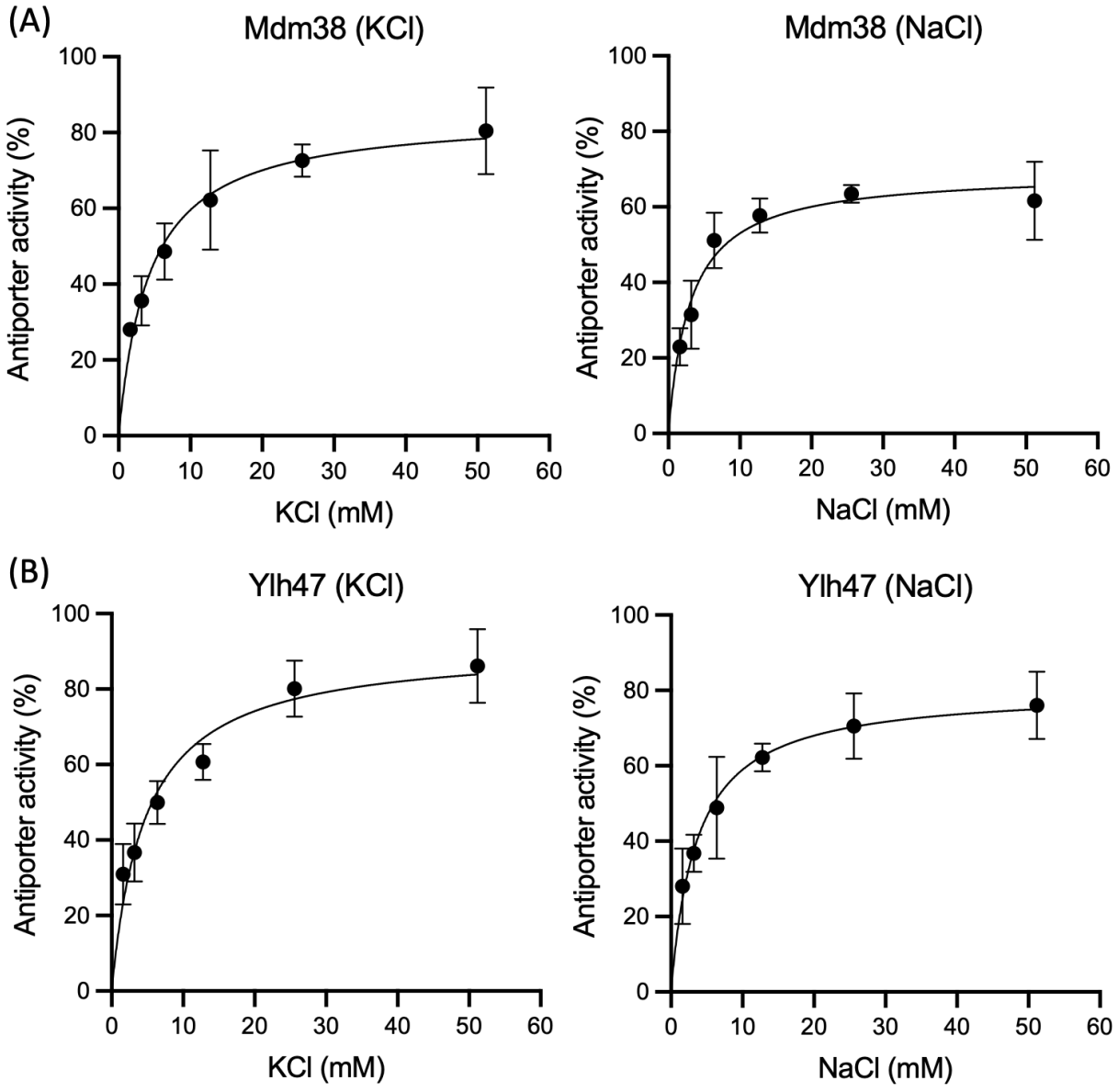

FIG 3 Michaelis-Menten kinetics of K^+/H^+ antiport and Na^+/H^+ antiport activities of Mdm38 and Ylh47 K^+/H^+ antiport activity and Na^+/H^+ antiport activity of Mdm38 (A) and Ylh47 (B) with varying concentrations of KCl or NaCl. The experiments were conducted by measuring dequenching of acridine orange fluorescence in inverted membranes as in Fig. 2. The error bars represent SD (n = 3) at different concentrations of KCl and NaCl.

region and CCs in the C-terminal region (Fig. S1). A glutamic acid residue (Glu221 in Letm1, Glu152 in Mdm38, and Glu150 in Ylh47) is conserved in the TM region of all three transporters (Fig. 5). Based on available data obtained from electron microscopy that show that Letm1 exists as a hexamer (10), a model structure for the protein family was created as a hexamer (Fig. 5). In the resulting model, the conserved glutamic acids are located next to the pore formed by the TM regions, with their side chains directed toward the center of the pore. *E. coli* NhaA, a canonical Na^+/H^+ antiporter, has aspartic acids in the center of its pore, which are essential for its Na^+/H^+ exchange activity (32). It seems likely that the negatively charged conserved glutamic acid may have a similar function in the Letm1-Mdm38-Ylh47 family. To clarify the role of this conserved glutamic acid in cation/H^+ antiport activity, we replaced the glutamic acid at position 152 in Mdm38 or at position 150 in Ylh47 with alanine and designated these variants Mdm38 E152A and Ylh47 E150A, respectively. Transformants of *E. coli* strain TO114 were then

TABLE 1 Kinetic parameters of Mdm38 and Ylh47[a]

	K_m (mM)	V_{max} (% fluorescence dequenching)
Mdm38 (KCl)	4.57 ± 1.94	85.93 ± 11.63
Mdm38 (NaCl)	3.41 ± 2.07	70.41 ± 9.64
Ylh47 (KCl)	4.79 ± 1.06	91.6 ± 5.88
Ylh47 (NaCl)	3.80 ± 1.19	80.56 ± 6.52

[a]Values are the averages and standard deviations of three biological replicates.

used in the same kind of growth assays as previously used for the wild-type proteins (see Fig. 1). As expected, Mdm38 and Ylh47 complemented the lack of growth of TO114 on medium with 25 mM NaCl and 10 µM IPTG (Fig. 6A) or 100 µM IPTG (Fig. 6B). In contrast, Mdm38 E152A and Ylh47 E150A failed to support growth on the same medium. Therefore, the Glu in the pore-forming region is likely to be required for the antiport activity in Mdm38 and Ylh47.

DISCUSSION

Examination of the ion transport activities of Mdm38 and Ylh47 revealed that they exchanged K^+, Na^+, and Li^+ for H^+; however, they did not have Ca^{2+}/H^+ antiport activity. This distinguishes Mdm38 and Ylh47 from Letm1, which possesses Ca^{2+}/H^+ antiport activity. Another distinction between Letm1 and Mdm38 and Ylh47 is the presence or absence of EF-hand domains (Fig. 4 and 7). The EF-hands in Letm1s are a component of calcium signaling (6, 7, 10, 11, 13). The measurements of K^+/H^+ antiport activity assay across the membranes of submitochondrial particles showed Mdm38 exhibits stoichiometries similar to those mediated by nigericin, which shows electroneutral K^+/H^+

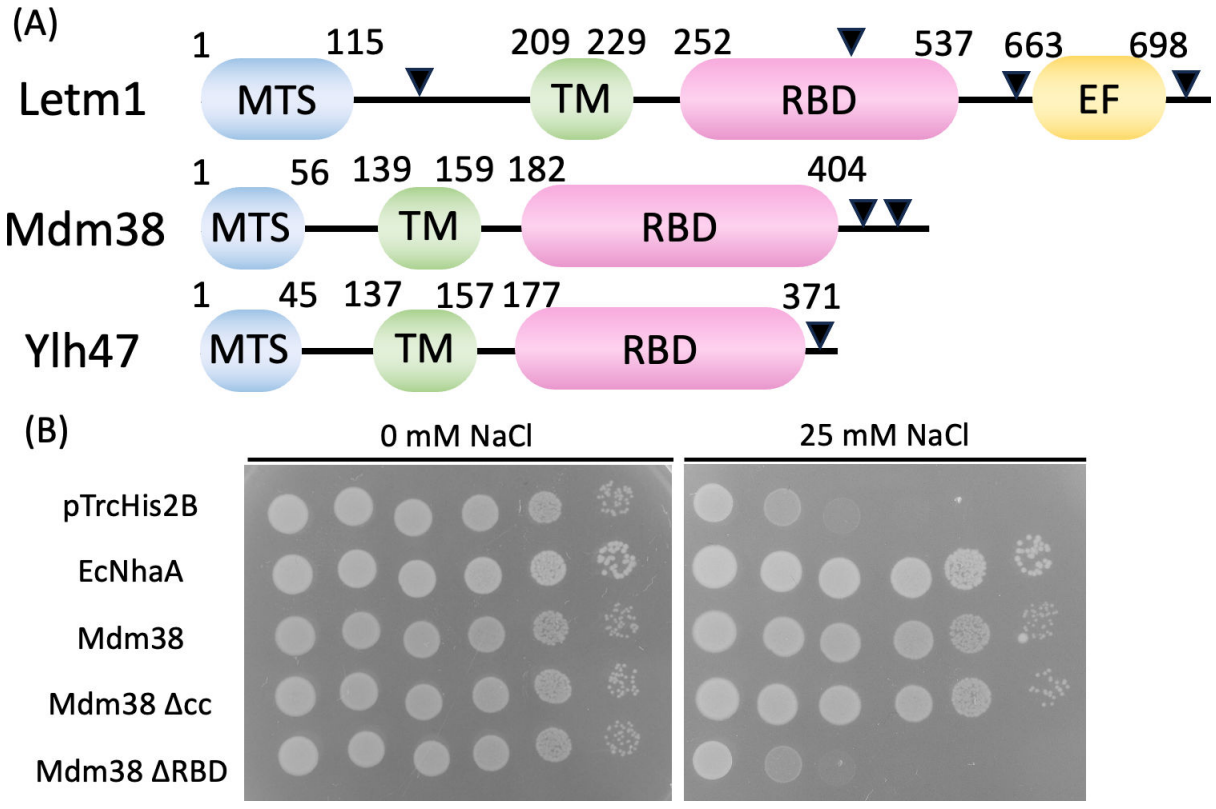

FIG 4 The C-terminal motif in Mdm38 is required for ion transport activity. (A) Model showing the predicted domains in Letm1, Mdm38, and Ylh47. EF, EF-hand domain. The black arrows indicate coiled-coil regions. (B) Complementation of salt sensitivity of *E. coli* TO114 by EcNhaA, Mdm38, Mdm38 ΔRBD, and Mdm38 Δcc. Tenfold serial dilutions of the cells were spotted on KLB containing 10 µM IPTG plus 0 mM or 25 mM NaCl. A representative example of three biological replicates is shown.

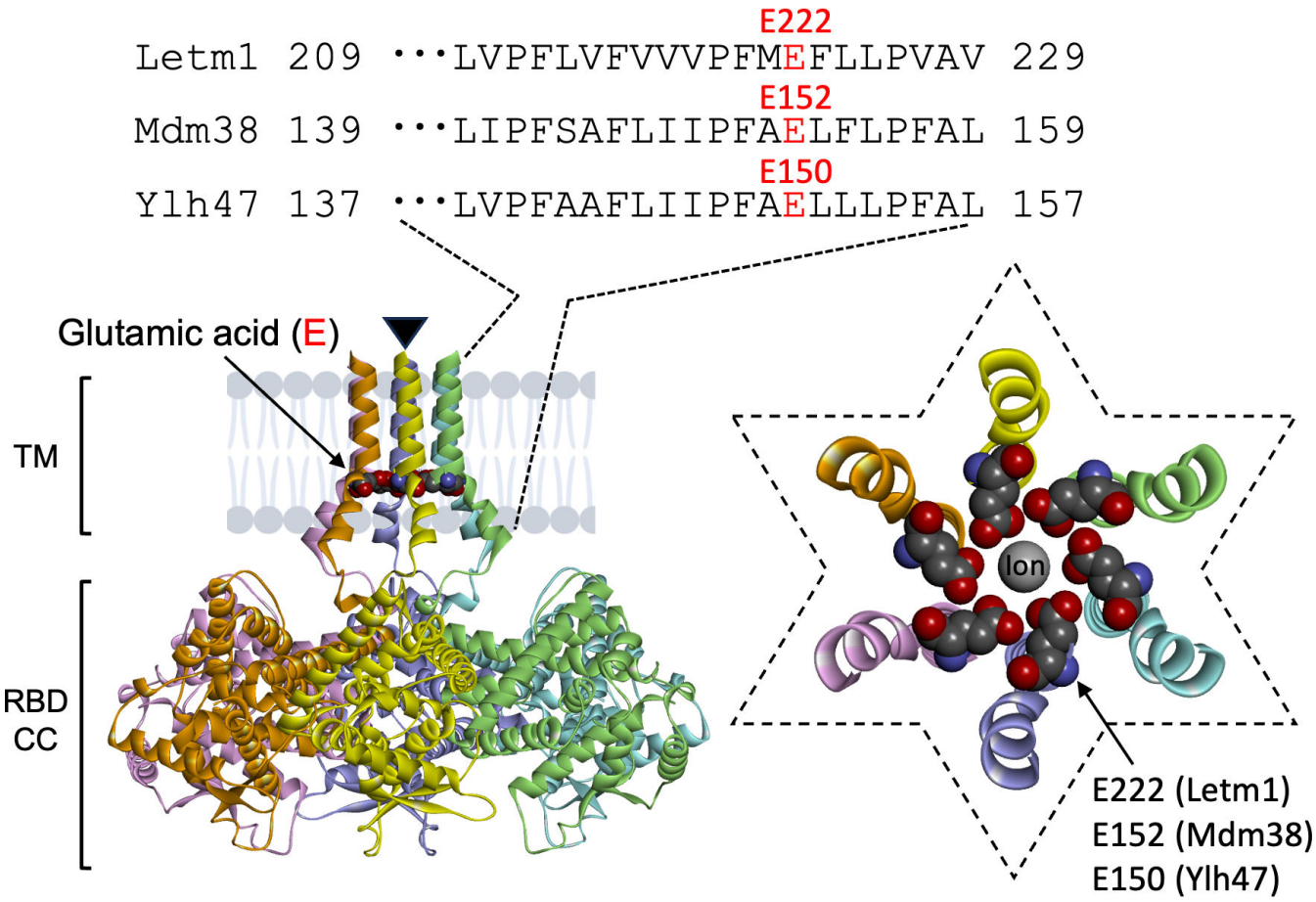

FIG 5 Structural model of Letm1, Mdm38, and Ylh47 showing the conserved glutamic acid in the transmembrane region. The amino acid sequence alignment of the transmembrane regions of Letm1, Mdm38, and Ylh47 is shown at the top, and the conserved glutamic acid is shown in red. The model at the bottom shows the structure for members of the Letm1-Mdm38-Ylh47 family as a hexamer. The side view is shown on the left, and the bottom view focused on the TM region (i.e., pore) on the right. The dashed six-pointed star approximates the shape of the RBDs (although the actual size would be much larger). The conserved glutamic acids are represented by red and gray spheres, with a bound ion at the center (manually placed).

antiport (18). These facts suggest that Letm1-mediated Ca^{2+}/H^+ exchanger and Mdm38/Ylh47-mediated monovalent/H^+ exchanger may have different contributions to the membrane potential across the inner mitochondrial membrane. Nevertheless, Letm1 and Letm1 variants lacking the EF-hand domains complement a yeast *mdm38* mutant (33). Furthermore, mitochondrial swelling assays also suggest that the knockdown of Letm1 decreases K^+/H^+ exchange activity across the inner mitochondrial membrane (34). These results suggest that Letm1 also retains K^+/H^+ exchange activity as well as Mdm38/Ylh47, and they may participate in maintaining mitochondrial monovalent cation homeostasis through their K^+/H^+ exchange activity. Mdm38 and Ylh47 also transported Na^+ in addition to K^+ (Fig. 2B). This is similar to thylakoid Na^+/H^+ antiporters in cyanobacteria, which are considered ancestors of chloroplasts. The model cyanobacteria strain, *Synechocystis* sp. PCC 6803, utilizes Na^+ in the medium and contains NhaS3, an Na^+/H^+ antiporter, that localizes to the thylakoid membrane which is the equivalent of the inner membrane of mitochondria (25). The *nhaS3* gene is essential for cell growth, and NhaS3-mediated Na^+/H^+ antiport activity is involved in electron transport across the thylakoid membrane. Similarly, Na^+/H^+ antiport by Mdm38 and Ylh47 may also contribute to maintain membrane potential in mitochondria of yeast. *Saccharomyces cerevisiae* possess Na^+ pump (ENA1) in the plasma membrane and Na^+/H^+ antiporter (NHX1) in the tonoplast (35, 36). Mdm38- and Ylh47-mediated Na^+/H^+ antiport activity

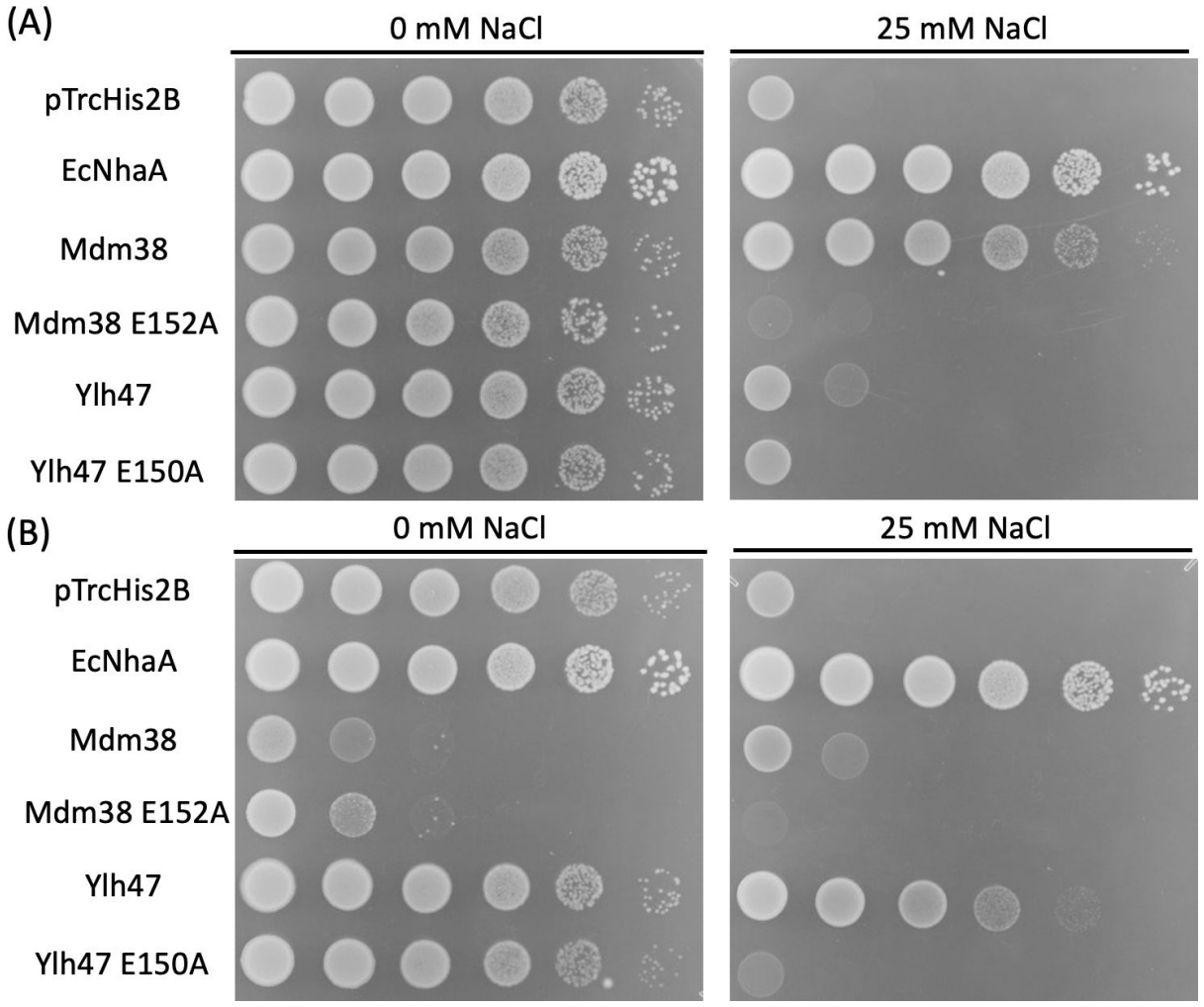

FIG 6 Ion transport activities of Mdm38 E152A and Ylh47 E150A. Growth assay of *E. coli* TO114 containing EcNhaA, Mdm38, Mdm38 E152A, Ylh47, or Ylh47 E150A on media with 0 or 25 mM NaCl. Tenfold serial dilutions of the cells were spotted on KLB containing 10 µM IPTG (A) or 100 µM IPTG (B).The representative data of three biological replicates are shown. A representative example of three biological replicates is shown.

may cooperatively function with them to control pH and alleviate Na^+ stress. In animal cells, glucose-dependent cytoplasmic Na^+ uptake is known to induce Na^+ influx into the mitochondrial matrix by Na^+/Ca^{2+} exchanger. It has been suggested that Na^+/H^+ antiporters can efflux Na^+ to counteract this Na^+ influx into the mitochondrial matrix (37). Likewise in yeast, Mdm38 and Ylh47 may efflux Na^+ from the matrix into the inter-membrane space when the Na^+ concentration in the mitochondrial matrix is elevated.

Both Ylh47 and Mdm38 are localized in the inner membrane of mitochondria in *S. cerevisiae* (16). However, the phenotype of the *ylh47* mutant is different from that of the *mdm38* mutant. Growth of the *ylh47* mutant on glycerol medium is similar to the wild type. Furthermore, the membrane potential of the inner mitochondrial membrane is unchanged, and the levels of proteins constituting complexes III and IV are unaffected in the *ylh47* mutant (16). On the other hand, overexpression of Ylh47 complements the delayed growth of the *mdm38* mutant in glycerol medium, and Ylh47 has also been shown to bind mitochondrial ribosomes, similar to Mdm38 (16, 17). The expression of Mdm38 conferred NaCl tolerance to the Na^+/H^+ antiport-deficient TO114 strain in media supplemented with 10µM IPTG, whereas Ylh47 did not (Fig. 1A). This suggested that Ylh47 might not exhibit sufficient transport activity when expressed at low levels, which may explain the phenotype of *mdm38* mutant when Ylh47 is overexpressed (16, 17).

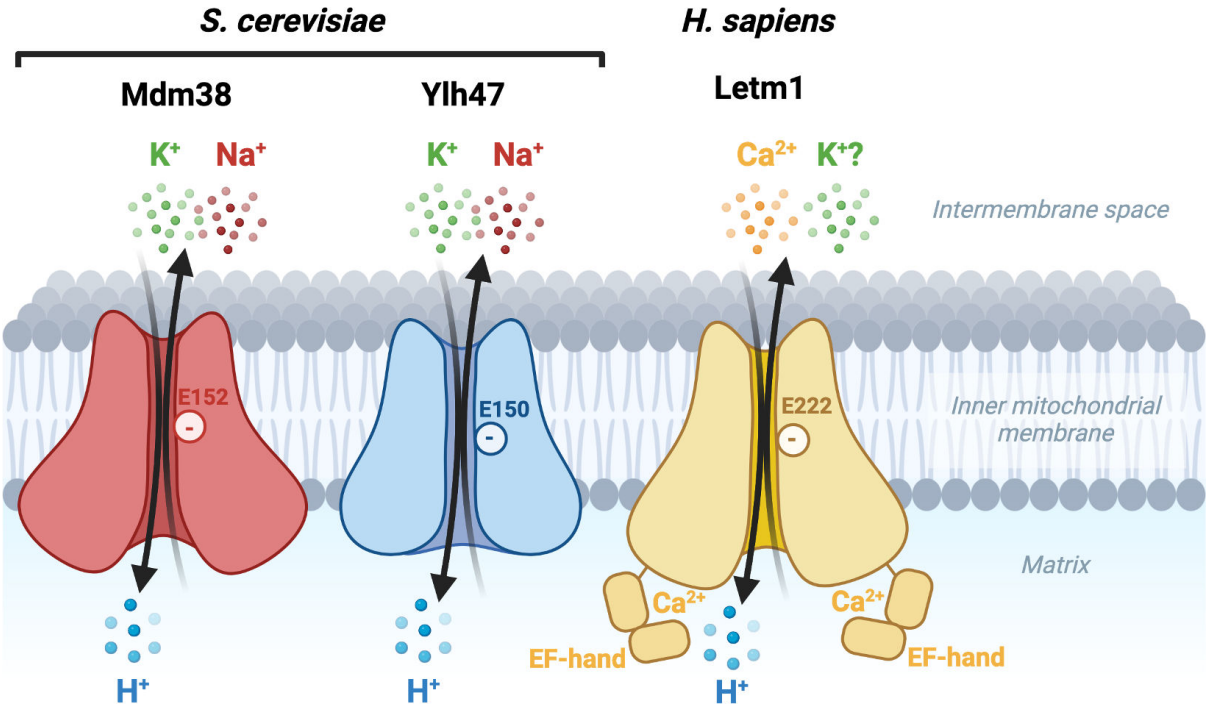

FIG 7 Comparison of cation/H^+ antiport activities and structures of Mdm38, Ylh47, and Letm1. LETM1, which has an EF-hand motif in its C-terminal region, has Ca^{2+}/H^+ antiport activity and also contributes to K^+/H^+ antiport activity. Mdm38 and Ylh47, which contain no EF-hand motif, showed K^+/H^+ and Na^+/H^+ antiport activity. The conserved glutamic acid residues in the transmembrane region of Mdm38 (E152), Ylh47 (E150), and Letm1 (E222) are labeled.

While the exact reason for the phenotypic differences between the *mdm38* and the *ylh47* mutant is unclear since both transporters have similar ion transport properties (Fig. 1 to 3 and 6), it is likely that differences in expression levels (Fig. 6) or regulatory systems may be contributing factors.

Mdm38 is known to have a dual role in both ion transport across the inner mitochondrial membrane and mitochondrial protein translation (16–18, 20–22). The transmembrane region is crucial for ion transport, while the RBD is responsible for the role in translation of mitochondrial proteins (20). The RBD occupies a large part of the C-terminal region (Fig. 4A), and deletion of the RBD from Mdm38 leads to impaired growth on glycerol medium and decreased abundance of proteins in the respiratory chain (20). Addition of the K^+/H^+ exchange ionophore nigericin does not complement the lack of RBD in Mdm38, suggesting that the RBD is important for protein translation. In our report, deletion of the RBD resulted in loss of ion transport activity of Mdm38 (Fig. 4B). These results suggested that RBD of Mdm38 is not only involved in translation of mitochondrial proteins but also in ion transport activity. Analysis of the crystal structure revealed that the RBD of Mdm38 is a 14-3-3-like domain, and these are known for their diverse protein interactions and formation of homo- and heterodimers (20, 38). Interaction between RBDs may enable the formation of the functional hexamer complex of Mdm38. Strains expressing Mdm38 lacking the CCs which are located at the end of the C-terminal region grow in glycerol medium at moderate temperatures but not at higher temperatures (20). Deletion of the CCs from Mdm38 does not affect its ability to bind to ribosomes, indicating that this domain is not required for ribosome binding (20). Consistent with this finding, expression of a Mdm38 variant lacking the CCs still complemented the Na^+ sensitivity of the TO114 strain (Fig. 4B). These data suggested that the CCs of Mdm38 did not contribute to ribosome binding or ion transport.

We identified a conserved glutamic acid in the middle of the transmembrane region in Mdm38 and Ylh47 and showed through structure modeling and growth complementation studies in *E. coli* that it is required for transport activity (Fig. 5 to 7). There is little

information on the cation/H^+ antiport mechanism of the Letm1-Mdm38-Ylh47 family (18), and the precise mechanism by which the six glutamic acids of a functional hexamer bind to cations and protons remains elusive. Participation of negatively charged residues in a cation/H^+ antiporter has been reported previously. The *E. coli* Na^+/H^+ antiporter NhaA has a DD motif that binds Na^+ and H^+ in the center of two funnel structures (32, 39). Similarly, K^+/H^+ antiporters, such as KefC in *E. coli* and KEA in *Arabidopsis*, have a conserved QD motif (24, 40). K^+ uptake transporters of the Kup/Ktr/HAK family contain conserved negatively charged residues in their transmembrane domains, and these residues are required for K^+ transport (41). Our biochemical analyses suggested that the negatively charged glutamic acid residues within the transmembrane regions were involved in transport activity, although their exact location and function still need to be confirmed by protein crystal structure analysis. Mdm38 and Ylh47 had the ability to transport a wide range of alkali metals, including Li^+, Na^+, K^+, and Rb^+, but they did not transport the divalent cation Ca^{2+} (Fig. 3). The amino acid sequences of the transmembrane regions of Mdm38, Ylh47, and Letm1 are relatively conserved, suggesting that the permeability of Ca^{2+} is regulated by specific amino acids. The K^+/H^+ antiport activity of Mdm38 contributes to membrane potential formation across the inner mitochondrial membrane (17).

This is similar to the role of KEA3, a K^+/H^+ antiporter localized to the thylakoid membrane of plant chloroplasts, which plays a role in light energy dissipation and membrane potential formation (24, 42, 43). Furthermore, an *Arabidopsis* mutant lacking chloroplast envelope-localized KEA1/2 and thylakoid-localized KEA3 exhibits swollen chloroplasts, similar to the mitochondria in the *mdm38* mutant (43). It is therefore likely that cation/H^+ antiporters contribute to similar kinds of intracellular events, such as protein synthesis, membrane potential formation, and morphogenesis in mitochondria, chloroplasts, and bacteria.

ACKNOWLEDGMENTS

We thank Saeko Tochigi and Erina Ishimaru for plasmid construction, and Anke Reinders for critical reading.

This work was supported by Grants-in-Aid for Scientific Research (20KK0127, 21H05266, 21KK0268, 22K19121, 23K13862, 24K08709, 24H00495, and 24H02253) from the Ministry of Education, Culture, Sports, Science and Technology, and Moonshot R&M (JPMJMS2033) from Japan Science and Technology Agency.

M.T., E.T., H.Z., H.S., A.K., and T.F. performed experiments; M.T. and N.U. designed this study and wrote the article; M.T., Y. I., and N.U. analyzed data. All authors approved the final article.

AUTHOR AFFILIATIONS

[1]Graduate School of Engineering, Tohoku University, Aobayama, Sendai, Japan
[2]School of Life Science and Technology, Tokyo Institute of Technology, Nagatsuta-cho, Yokohama, Japan

AUTHOR ORCIDs

Masaru Tsujii http://orcid.org/0000-0003-2127-1988
Tadaomi Furuta http://orcid.org/0000-0003-4568-9043
Nobuyuki Uozumi http://orcid.org/0000-0003-4268-1126

FUNDING

Funder	Grant(s)	Author(s)
MEXT | Japan Society for the Promotion of Science (JSPS)	20KK0127	Nobuyuki Uozumi

Funder	Grant(s)	Author(s)
MEXT | Japan Society for the Promotion of Science (JSPS)	21H05266	Yasuhiro Ishimaru
MEXT | Japan Society for the Promotion of Science (JSPS)	21KK0268	Yasuhiro Ishimaru
MEXT | Japan Society for the Promotion of Science (JSPS)	22K19121	Yasuhiro Ishimaru
MEXT | Japan Society for the Promotion of Science (JSPS)	23K13862	Ellen Tanudjaja
MEXT | Japan Society for the Promotion of Science (JSPS)	24K08709	Masaru Tsujii
MEXT | Japan Society for the Promotion of Science (JSPS)	24H00495	Nobuyuki Uozumi
MEXT | Japan Society for the Promotion of Science (JSPS)	24H02253	Nobuyuki Uozumi
MEXT | Japan Science and Technology Agency (JST)	JPMJMS2033	Nobuyuki Uozumi

AUTHOR CONTRIBUTIONS

Masaru Tsujii, Data curation, Formal analysis, Funding acquisition, Methodology, Resources, Supervision, Validation, Writing – original draft | Ellen Tanudjaja, Formal analysis, Funding acquisition, Methodology, Visualization, Writing – review and editing | Haoyu Zhang, Formal analysis, Validation, Writing – review and editing | Haruto Shimizukawa, Formal analysis, Validation | Ayumi Konishi, Formal analysis | Tadaomi Furuta, Data curation, Formal analysis, Visualization, Writing – original draft | Yasuhiro Ishimaru, Writing – review and editing | Nobuyuki Uozumi, Conceptualization, Data curation, Funding acquisition, Investigation, Project administration, Supervision, Validation, Writing – original draft, Writing – review and editing

ADDITIONAL FILES

The following material is available online.

Supplemental Material

Figure S1 and Table S1 (JB00182-24-s0001.pdf). Sequence alignment, and primers used in this study.

REFERENCES

1. EthertonB, HiginbothamN. 1960. Transmembrane potential measurements of cells of higher plants as related to salt uptake. Science 131:409–410. https://doi.org/10.1126/science.131.3398.409
2. Cheeseman JM, Hanson JB. 1979. Mathematical analysis of the dependence of cell potential on external potassium in corn roots. Plant Physiol 63:1–4. https://doi.org/10.1104/pp.63.1.1
3. Maathuis F, Sanders D. 1993. Energization of potassium uptake in *Arabidopsis thaliana*. Planta 191:302–307. https://doi.org/10.1007/BF00195686
4. Bernardi P. 1999. Mitochondrial transport of cations: channels, exchangers, and permeability transition. Physiol Rev 79:1127–1155. https://doi.org/10.1152/physrev.1999.79.4.1127
5. MitchellP. 1961. Coupling of phosphorylation to electron and hydrogen transfer by a chemi-osmotic type of mechanism. Nature 191:144–148. https://doi.org/10.1038/191144a0
6. Endele S, Fuhry M, Pak SJ, Zabel BU, Winterpacht A. 1999. LETM1, a novel gene encoding a putative EF-hand Ca^{2+}-binding protein, flanks the Wolf-Hirschhorn syndrome (WHS) critical region and is deleted in most WHS patients. Genomics 60:218–225. https://doi.org/10.1006/geno.1999.5881
7. Jiang D, Zhao L, Clapham DE. 2009. Genome-wide RNAi screen identifies Letm1 as a mitochondrial Ca^{2+}/H^{+} antiporter. Science 326:144–147. https://doi.org/10.1126/science.1175145
8. McQuibban AG, Joza N, Megighian A, Scorzeto M, Zanini D, Reipert S, Richter C, Schweyen RJ, Nowikovsky K. 2010. A *Drosophila* mutant of LETM1, a candidate gene for seizures in Wolf-Hirschhorn syndrome. Hum Mol Genet 19:987–1000. https://doi.org/10.1093/hmg/ddp563
9. Piao L, Li Y, Kim SJ, Sohn K-C, Yang K-J, Park KA, Byun HS, Won M, Hong J, Hur GM, Seok JH, Shong M, Sack R, Brazil DP, Hemmings BA, Park J. 2009. Regulation of OPA1-mediated mitochondrial fusion by leucine zipper/EF-hand-containing transmembrane protein-1 plays a role in apoptosis. Cell Signal 21:767–777. https://doi.org/10.1016/j.cellsig.2009.01.020
10. Shao J, Fu Z, Ji Y, Guan X, Guo S, Ding Z, Yang X, Cong Y, Shen Y. 2016. Leucine zipper-EF-hand containing transmembrane protein 1 (LETM1) forms a Ca^{2+}/H^{+} antiporter. Sci Rep 6:34174. https://doi.org/10.1038/srep34174
11. Tsai M-F, Jiang D, Zhao L, Clapham D, Miller C. 2014. Functional reconstitution of the mitochondrial Ca^{2+}/H^{+} antiporter Letm1. J Gen Physiol 143:67–73. https://doi.org/10.1085/jgp.201311096

12. Doonan PJ, Chandramoorthy HC, Hoffman NE, Zhang X, Cárdenas C, Shanmughapriya S, Rajan S, Vallem S, Chen X, Foskett JK, Cheung JY, Houser SR, Madesh M. 2014. LETM1-dependent mitochondrial Ca^{2+} flux modulates cellular bioenergetics and proliferation. FASEB J 28:4936–4949. https://doi.org/10.1096/fj.14-256453
13. Jiang D, Zhao L, Clish CB, Clapham DE. 2013. Letm1, the mitochondrial Ca^{2+}/H^{+} antiporter, is essential for normal glucose metabolism and alters brain function in Wolf-Hirschhorn syndrome. Proc Natl Acad Sci U S A 110:E2249–E2254. https://doi.org/10.1073/pnas.1308558110
14. Hasegawa A, van der Bliek AM. 2007. Inverse correlation between expression of the Wolfs Hirschhorn candidate gene Letm1 and mitochondrial volume in *C. elegans* and in mammalian cells. Hum Mol Genet 16:2061–2071. https://doi.org/10.1093/hmg/ddm154
15. Hashimi H, McDonald L, Stríbrná E, Lukeš J. 2013. Trypanosome Letm1 protein is essential for mitochondrial potassium homeostasis. J Biol Chem 288:26914–26925. https://doi.org/10.1074/jbc.M113.495119
16. Frazier AE, Taylor RD, Mick DU, Warscheid B, Stoepel N, Meyer HE, Ryan MT, Guiard B, Rehling P. 2006. Mdm38 interacts with ribosomes and is a component of the mitochondrial protein export machinery. J Cell Biol 172:553–564. https://doi.org/10.1083/jcb.200505060
17. Nowikovsky K, Froschauer EM, Zsurka G, Samaj J, Reipert S, Kolisek M, Wiesenberger G, Schweyen RJ. 2004. The *LETM1/YOL027* gene family encodes a factor of the mitochondrial K^{+} homeostasis with a potential role in the Wolf-Hirschhorn syndrome. J Biol Chem 279:30307–30315. https://doi.org/10.1074/jbc.M403607200
18. Froschauer E, Nowikovsky K, Schweyen RJ. 2005. Electroneutral K^{+}/H^{+} exchange in mitochondrial membrane vesicles involves Yo1027/Letm1 proteins. Biochim Biophys Acta 1711:41–48. https://doi.org/10.1016/j.bbamem.2005.02.018
19. Nowikovsky K, Reipert S, Devenish RJ, Schweyen RJ. 2007. Mdm38 protein depletion causes loss of mitochondrial K^{+}/H^{+} exchange activity, osmotic swelling and mitophagy. Cell Death Differ 14:1647–1656. https://doi.org/10.1038/sj.cdd.4402167
20. Lupo D, Vollmer C, Deckers M, Mick DU, Tews I, Sinning I, Rehling P. 2011. Mdm38 is a 14-3-3-like receptor and associates with the protein synthesis machinery at the inner mitochondrial membrane. Traffic 12:1457–1466. https://doi.org/10.1111/j.1600-0854.2011.01239.x
21. Bauerschmitt H, Mick DU, Deckers M, Vollmer C, Funes S, Kehrein K, Ott M, Rehling P, Herrmann JM. 2010. Ribosome-binding proteins Mdm38 and Mba1 display overlapping functions for regulation of mitochondrial translation. Mol Biol Cell 21:1937–1944. https://doi.org/10.1091/mbc.e10-02-0101
22. Zotova L, Aleschko M, Sponder G, Baumgartner R, Reipert S, Prinz M, Schweyen RJ, Nowikovsky K. 2010. Novel components of an active mitochondrial K^{+}/H^{+} exchange. J Biol Chem 285:14399–14414. https://doi.org/10.1074/jbc.M109.059956
23. Ohyama T, Igarashi K, Kobayashi H. 1994. Physiological role of the chaA gene in sodium and calcium circulations at a high pH in *Escherichia coli*. J Bacteriol 176:4311–4315. https://doi.org/10.1128/jb.176.14.4311-4315.1994
24. Tsujii M, Kera K, Hamamoto S, Kuromori T, Shikanai T, Uozumi N. 2019. Evidence for potassium transport activity of Arabidopsis KEA1-KEA6. Sci Rep 9:10040. https://doi.org/10.1038/s41598-019-46463-7
25. Tsunekawa K, Shijuku T, Hayashimoto M, Kojima Y, Onai K, Morishita M, Ishiura M, Kuroda T, Nakamura T, Kobayashi H, Sato M, Toyooka K, Matsuoka K, Omata T, Uozumi N. 2009. Identification and characterization of the Na^{+}/H^{+} antiporter NhaS3 from the thylakoid membrane of *Synechocystis* sp. PCC 6803. J Biol Chem 284:16513–16521. https://doi.org/10.1074/jbc.M109.001875
26. Harada K, Arizono T, Sato R, Trinh MDL, Hashimoto A, Kono M, Tsujii M, Uozumi N, Takaichi S, Masuda S. 2019. DAY-LENGTH-DEPENDENT DELAYED-GREENING1, the Arabidopsis homolog of the cyanobacterial H^{+}-extrusion protein, is essential for chloroplast pH regulation and optimization of non-photochemical quenching. Plant Cell Physiol 60:2660–2671. https://doi.org/10.1093/pcp/pcz203
27. Tanudjaja E, Hoshi N, Yamamoto K, Ihara K, Furuta T, Tsujii M, Ishimaru Y, Uozumi N. 2023. Two Trk/Ktr/HKT-type potassium transporters, TrkG and TrkH, perform distinct functions in *Escherichia coli* K-12. J Biol Chem 299:102846. https://doi.org/10.1016/j.jbc.2022.102846
28. Kuroda T, Shimamoto T, Inaba K, Kayahara T, Tsuda M, Tsuchiya T. 1994. Properties of the Na^{+}/H^{+} antiporter in *Vibrio parahaemolyticus*. J Biochem 115:1162–1165. https://doi.org/10.1093/oxfordjournals.jbchem.a124473
29. Sievers F, Higgins DG. 2021. The clustal omega multiple alignment package. Methods Mol Biol 2231:3–16. https://doi.org/10.1007/978-1-0716-1036-7_1
30. Jacques DA, McEwan WA, Hilditch L, Price AJ, Towers GJ, James LC. 2016. HIV-1 uses dynamic capsid pores to import nucleotides and fuel encapsidated DNA synthesis. Nature 536:349–353. https://doi.org/10.1038/nature19098
31. Uozumi N. 2001. *Escherichia coli* as an expression system for K^{+} transport systems from plants. Am J Physiol Cell Physiol 281:C733–C739. https://doi.org/10.1152/ajpcell.2001.281.3.C733
32. Hunte C, Screpanti E, Venturi M, Rimon A, Padan E, Michel H. 2005. Structure of a Na^{+}/H^{+} antiporter and insights into mechanism of action and regulation by pH. Nature 435:1197–1202. https://doi.org/10.1038/nature03692
33. Nakamura S, Matsui A, Akabane S, Tamura Y, Hatano A, Miyano Y, Omote H, Kajikawa M, Maenaka K, Moriyama Y, Endo T, Oka T. 2020. The mitochondrial inner membrane protein LETM1 modulates cristae organization through its LETM domain. Commun Biol 3:99. https://doi.org/10.1038/s42003-020-0832-5
34. Austin S, Mekis R, Mohammed SEM, Scalise M, Wang WA, Galluccio M, Pfeiffer C, Borovec T, Parapatics K, Vitko D, Dinhopl N, Demaurex N, Bennett KL, Indiveri C, Nowikovsky K. 2022. TMBIM5 is the $Ca2^{+}/H^{+}$ antiporter of mammalian mitochondria. EMBO Rep 23:e54978. https://doi.org/10.15252/embr.202254978
35. Bañuelos MA, Quintero FJ, Rodríguez-Navarro A. 1995. Functional expression of the ENA1(PMR2)-ATPase of *Saccharomyces cerevisiae* in *Schizosaccharomyces pombe*. Biochim Biophys Acta 1229:233–238. https://doi.org/10.1016/0005-2728(95)00006-5
36. Nass R, Cunningham KW, Rao R. 1997. Intracellular sequestration of sodium by a novel Na^{+}/H^{+} exchanger in yeast is enhanced by mutations in the plasma membrane H^{+}-ATPase. Insights into mechanisms of sodium tolerance. J Biol Chem 272:26145–26152. https://doi.org/10.1074/jbc.272.42.26145
37. Nita II, Hershfinkel M, Lewis EC, Sekler I. 2015. A crosstalk between Na^{+} channels, Na^{+}/K^{+} pump and mitochondrial Na^{+} transporters controls glucose-dependent cytosolic and mitochondrial Na^{+} signals. Cell Calcium 57:69–75. https://doi.org/10.1016/j.ceca.2014.12.007
38. Yang X, Lee WH, Sobott F, Papagrigoriou E, Robinson CV, Grossmann JG, Sundström M, Doyle DA, Elkins JM. 2006. Structural basis for protein-protein interactions in the 14-3-3 protein family. Proc Natl Acad Sci U S A 103:17237–17242. https://doi.org/10.1073/pnas.0605779103
39. Tsujii M, Tanudjaja E, Uozumi N. 2020. Diverse physiological functions of cation proton antiporters across bacteria and plant cells. Int J Mol Sci 21:4566. https://doi.org/10.3390/ijms21124566
40. Aranda-Sicilia MN, Cagnac O, Chanroj S, Sze H, Rodríguez-Rosales MP, Venema K. 2012. *Arabidopsis* KEA2, a homolog of bacterial KefC, encodes a K^{+}/H^{+} antiporter with a chloroplast transit peptide. Biochim Biophys Acta 1818:2362–2371. https://doi.org/10.1016/j.bbamem.2012.04.011
41. Sato Y, Nanatani K, Hamamoto S, Shimizu M, Takahashi M, Tabuchi-Kobayashi M, Mizutani A, Schroeder JI, Souma S, Uozumi N. 2014. Defining membrane spanning domains and crucial membrane-localized acidic amino acid residues for K^{+} transport of a Kup/HAK/KT-type *Escherichia coli* potassium transporter. J Biochem 155:315–323. https://doi.org/10.1093/jb/mvu007
42. Armbruster U, Carrillo LR, Venema K, Pavlovic L, Schmidtmann E, Kornfeld A, Jahns P, Berry JA, Kramer DM, Jonikas MC. 2014. Ion antiport accelerates photosynthetic acclimation in fluctuating light environments. Nat Commun 5:5439. https://doi.org/10.1038/ncomms6439
43. Kunz H-H, Gierth M, Herdean A, Satoh-Cruz M, Kramer DM, Spetea C, Schroeder JI. 2014. Plastidial transporters KEA1, -2, and -3 are essential for chloroplast osmoregulation, integrity, and pH regulation in *Arabidopsis*. Proc Natl Acad Sci U S A 111:7480–7485. https://doi.org/10.1073/pnas.1323899111